A stochastic modelling approach for the characterisation of collision exchange processes

Chunbing Huang[1], Federica Cattani[2], Patrick M. Piccione[3,◇], and Federico Galvanin[1,*]

[1]*Department of Chemical Engineering, University College London, Gower Street, London WC1E 6BT, UK*
[2]*Process Studies Group, Global Sourcing and Production, Syngenta, Jealott's Hill International Research Centre, Bracknell, Berkshire RG42 6EY, UK*
[3]*Syngenta, 4333 Münchwilen, Switzerland*
[◇]*Current address: F. Hoffmann-La Roche AG, 4070 Basel, Switzerland*
[*]*f.galvanin@ucl.ac.uk*

Abstract

Collision-exchange process is a common physical process where system members interact with each other to exchange materials and these individual interactions cumulatively drive a macroscopic system evolution in time. In this paper, a compartment-based stochastic model is formulated to study the collision-exchange process between members in a system. The discrete Markov analysis on the stochastic model presents the analytical results that show the independence of the system equilibrium on its initial distribution, and the derived differential equations reveal the deterministic time evolution of material amount on system members. As a specific example of a physical system that can be described via this model, a seed coating process is presented where the inter-particle coating variability is expressed by the stochastic model parameters. The promising agreement between simulation predictions and experimental results demonstrates the feasibility of stochastic modelling on the collision-exchange process and facilitates further model identification and applications to industrial processes.

Keywords: Collision-exchange process, compartment-based modelling, stochastic simulation, stochastic Markov process, seed coating system

1 Introduction

Collision-exchange process is a common physical process that arises in many systems where system members interact to engender material transfers or information exchange over the population. The nature of collision-exchange process in thermodynamic systems can be reflected by the energy exchange process between neighbouring particles, leading to a thermal conduction throughout the model grid [1]. In epidemiology, the interaction behaviour is mathematically formulated to study the spread of infections and diseases that may lead to an outbreak as a result of individual contacts [2, 3]. In chemical reaction-diffusion systems with low molecule concentration, molecules are formulated to react when they come across and consequently lead to population changes in reactants and products [4, 5]. In particle coating processes, coating liquid is transferred between particles as a consequence of particle contacts [6].

To understand the evolution of such systems and to obtain a quantitative distribution of exchanged material, it is essential to simulate the collision-exchange process assuming proper operation conditions and interaction mechanism. For chemical reaction-diffusion systems [4, 5] with very small elements (i.e. molecules) or pandemic models [3, 7] with large elements (i.e. humans), stochastic modelling has been widely employed to investigate the time-dependent system evolution dynamically driven by successive member interactions. Conversely, discrete element method (DEM) is commonly used to simulate the collision-exchange behaviour of system members, especially for granular particle systems [8–10]. For such systems with elements of intermediate size, very

few studies have investigated the system state and its evolution using stochastic modelling approach. The most challenging part in DEM simulations of these systems is to adequately trace each independent particle and change its system state within each numerical time interval, which is computationally demanding, especially for systems with large population size. Besides, particle collisions in DEM simulations usually involve the analysis of elastic [11] and inelastic [12] collisions, to increase the simulation precision by sacrificing computational efficiency. Consequently, DEM simulations require sufficiently long time to complete and produce results, which is not conducive to further model identification and system optimisation. Due to these limitations, DEM is not usually adopted as an approach for process optimisation unless advanced computing resources, such as large computer clusters and powerful graphical processing units, are available. Compared to the DEM, a stochastic modelling approach is more flexible and simulation time-saving. It assumes complex particle behaviour as random behaviour, regardless of elastic or inelastic collision, by applying a lower number of parameters and resultant low computational intensity, giving much convenience to quantitatively characterise simulation outcomes.

In this paper, a stochastic modelling approach by formulating a compartment-based stochastic model is applied to investigate a system with collision-exchange processes with the goal to characterise the state evolution by material distribution. The model is mainly concerned with the exchange behaviour between system members. Material distribution is used as a specific application of the model. To simulate the model, Gillespie's stochastic simulation algorithm (SSA) [4] is used to numerically compute the state change of the system. An illustrative example related to a seed coating process is given to present the feasibility of the model in practical use.

The paper is structured as follows. In Section 2, a 3D stochastic model is formulated with essential assumptions to implement the collision-exchange processes. In this section, we will discuss the properties of the stochastic model and give a deterministic approximation of the system evolution. In Section 3, stochastic simulations are presented based on an industrial example of seed coating process, with comparisons of simulations and experiments. Conclusions are presented in Section 4.

2 Methodology

Stochastic models built for molecular and epidemiological systems describe the system process in terms of model equations considering the nature of system uncertainty. Unlike DEM simulations giving the same output from unchanged operating conditions, stochastic modelling is inherently random. Repeating a simulation with the same conditions allows to explore the variability of the prediction. From these different simulation realisations, an ensemble of model outputs including uncertainty provides the statistic information missing from deterministic models.

2.1 Stochastic modelling on neighbouring collision-exchange process

A compartment-based model is formulated to represent collisions between neighbouring particles as illustrated by Figure 1. A 3D spatial domain is divided into compartments with one particle in each compartment. The numbers of compartments in x, y and z dimensions are K_x, K_y and K_z, respectively. It is postulated that every cubic compartment contains a single spheric particle of the same size in diameter and is confined within this subvolume. We assume that each particle tends to stay in its own compartment and the neighbours behave as barriers to prevent the particle to travel into another compartment, that is to say, the order of particles remains unchanged in the model. To illustrate the collision-exchange process between particles from two neighbouring compartments, the compartments and the inside particles are denoted by the following index set

$$\begin{aligned} I_{all} = \{(i,j,k) \mid i,j,k \in \mathbb{Z}, \\ 1 \leqslant i \leqslant K_x, 1 \leqslant j \leqslant K_y, 1 \leqslant k \leqslant K_z\} \end{aligned} \tag{1}$$

The confined particles are assumed to collide with their neighbours in only non-diagonal directions. We define the following set of collision directions by which one particle may contact one of its non-diagonal neighbours

$$\begin{aligned} E = \{&(-1,0,0),(1,0,0), \\ &(0,-1,0),(0,1,0), \\ &(0,0,-1),(0,0,1)\} \\ = \{&\mathbf{x}-,\mathbf{x}+, \\ &\mathbf{y}-,\mathbf{y}+, \\ &\mathbf{z}-,\mathbf{z}+\} \end{aligned} \tag{2}$$

The non-diagonal neighbours of the particle in the (i,j,k)-th compartment are defined by the following set

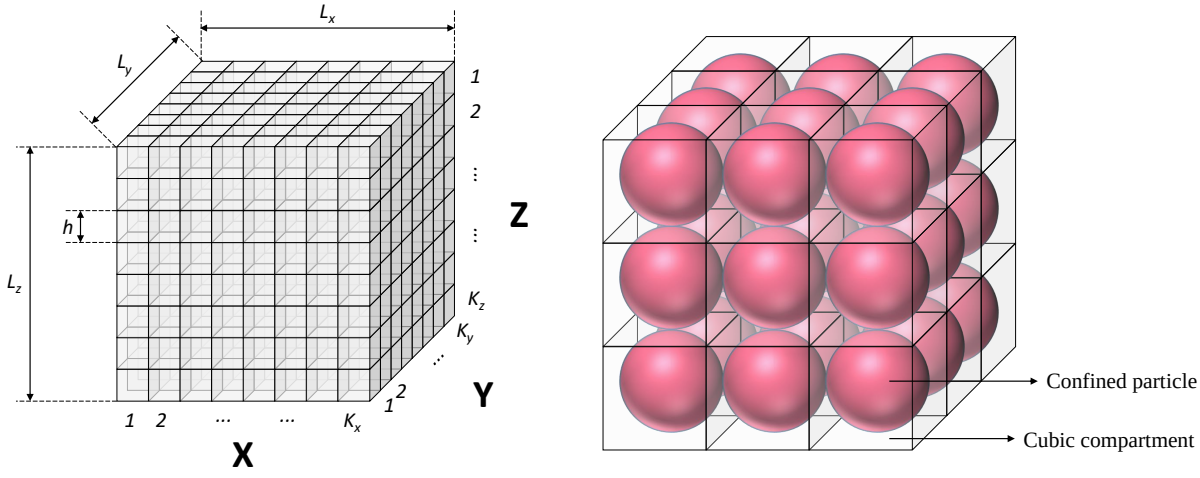

(a) (b)

Figure 1: (a) Discretisation of a 3D spatial domain $L_x \times L_y \times L_z$ by cubic compartments of the same edge length h. The domain with the number of compartments in each dimension $K_x = K_y = K_z = 8$ is shown on the figure; (b) Single particle is confined in each cubic compartment where the particle has limited space to move.

where **e** represents the direction of one of the neighbouring particles.

$$N_{i,j,k} = \{(i,j,k) + \mathbf{e} \,|\, (i,j,k) + \mathbf{e} \in I_{all},\ \mathbf{e} \in E\} \quad (3)$$

Particle contact frequency

A collision is required for an extensive physical property to be transferred between particles. A specific example is the exchange of mass. Let c_f (s^{-1}) denote the contact frequency to characterise the total number of particle contacts per second in the system. It is reasonable to assume that c_f stays constant by neglecting potential slight fluctuation when the system achieves dynamic equilibrium. In this model we do not consider the contact frequency of a single particle because particles at different positions can have different contact frequencies. Tracking every particle individually would increase computational expense in simulations.

Material transfer mechanism

Focusing on the specific example of material transfer, upon each collision involving two particles, see Figure 2, it is considered that one particle would both *give* and *receive* material from the other particle, forming an exchange event. Let $m_{i,j,k}(t)$ and $m_{(i,j,k)+\mathbf{e}}(t)$ denote respectively the material amount on the (i,j,k)-th particle and one of its neighbour $(i,j,k) + \mathbf{e}$ at time t. For the (i,j,k)-th particle colliding with the neighbour $(i,j,k)+\mathbf{e}$, we define the following expression to represent the material amount change involving two particles in the exchange event at time t,

$$\begin{aligned} m_{i,j,k}(t+\Delta t) - m_{i,j,k}(t) & \\ = -m_{i,j,k}(t)K_A + m_{(i,j,k)+\mathbf{e}}(t)K_P & \quad (4) \\ \{(i,j,k),(i,j,k)+\mathbf{e}\} \subset I_{all},\ \mathbf{e} \in E & \end{aligned}$$

where K_A represents the material amount fraction transferred from the particle (i,j,k) to its selected neighbour $(i,j,k)+\mathbf{e}$ and K_P from the selected neighbour to the particle. Δt represents the numerical computational time interval which will be discussed later. In this model, we assume that the material transferred is determined only by the material amount on the involved particles and the transfer coefficients. To simplify the model, we consider a process for which K_A and K_P can be considered as constant (no strong variation of physical properties during the process). The exchange process (4) is a stochastic process for the (i,j,k)-th particle as its neighbour selected from the set $N_{i,j,k}$ is completely random. Later we will show how we can implement a stochastic simulation algorithm based on this exchange mechanism.

Computational time interval

After introducing the material transfer mechanism above, the numerical time step, denoted as Δt, needs to be discussed. The value of Δt applied in the simulation is dependent on two critical factors of the system: collision frequency c_f and particle population K. One needs to consider the following constraints when selecting of an appropriate value of Δt.

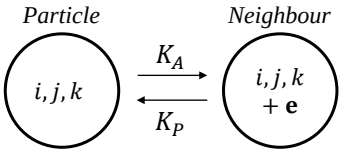

Figure 2: Illustration of a two-particle collision involving particle (i, j, k) and its neighbour $(i, j, k) + \mathbf{e}$.

- Δt is required not to be larger than $K/2c_f$. Once $c_f\Delta t > K/2$, the simulation goes to failure as there would be not enough particles left to be neighbours.
- Δt should not be too small. When $c_f\Delta t \ll 1$, the simulation would risk "nothing happens" for a lot of the time, which makes the simulation progress extremely slowly.
- $c_f\Delta t$ should not be close to $K/2$ as it "forces" $c_f\Delta t$ selected particles to collide at the same time (every particle is independent in the system).

With these considerations, it is actually required a trade-off between acceptable simulation time and forcing as less particles to collide at the same time as possible. To apply decent and reliable value of Δt, in this paper, we use a value selection criterion for Δt that $1 \leqslant c_f\Delta t < K/10$ where the randomly selected $c_f\Delta t$ particles and $c_f\Delta t$ corresponding neighbours per iteration account for only a small part of all particles in the system, ensuring the simulations can be completed with reasonable computational time and high reliability.

Collision propensity

During a small time interval, the particles need to "*choose*" with which neighbour they would collide and therefore exchange. This decision is related to the external forces, like gravitational force and centrifugal force applied on the particles. In this stochastic model, instead of determining collision directions based on Newtonian models (like in DEM simulations), we introduce the concept of "collision propensity" to characterise the probabilities that the particles would contact their neighbour in a specific direction. Let $P^{\mathbf{e}}_{i,j,k}$ denote the collision propensity for the (i, j, k)-th particle in the direction $\mathbf{e}$. Evidently, we have

$$\sum_{\mathbf{e}\in E} P^{\mathbf{e}}_{i,j,k} = 1 \tag{5}$$

Stochastic simulation algorithm

Prompted with considerations above, the stochastic simulation algorithm of the particle collision-exchange process is implemented as follows:

1. *Initialise the model with the following model parameters* $\theta = [K_A, K_P, c_f]^T$ *and simulation settings* $P^{\mathbf{e}}_{i,j,k}$, Δt, T_{total} *and* $t_{sampling}$;
2. *Record the system status every* $t_{sampling}$ *seconds;*
3. *Randomly select* $c_f\Delta t$ *particles from the model;*
4. *Randomly select* $c_f\Delta t$ *neighbours for the selected particles;*
5. *Calculate the material change amount on all selected particles and their involved neighbours;*
6. *Update the material of the corresponding particles based on Equation* (4) *to reflect particle exchange processes; set* $t \leftarrow t + \Delta t$;
7. *Go to step 2 if* $t < T_{total}$.

2.1.1 Stochastic model property

a. Property of the stochastic process

In this section, we investigate the discrete stochastic process associated with the collision-exchange system via a hidden stochastic Markov chain [13]. A Markov chain analysis produces insight on the fundamental properties of the system without running complex simulations. In fact, it elucidates how simulations are expected to behave offering a test for their validity.

Let us label the particles in the model from 1 to N, the system state at time t with respect to the material amount on all particles are denoted by

$$\mathbf{s}(t)^T = \left(s_1^{(t)}, \cdots, s_l^{(t)}, \cdots, s_N^{(t)}\right) \quad 1 \leqslant l \leqslant N \tag{6}$$

where $s_l^{(t)}$ represents the material amount on the particle labelled by l at time t. The system state at time t can be obtained by updating the system state computed at time $t - \Delta t$ and Equation (4) is rewritten in matrix form.

$$\mathbf{s}(t)^T = \mathbf{s}(t - \Delta t)^T\mathbf{P}_t \tag{7}$$

where $\mathbf{P}_t \in \mathbb{R}^{N\times N}$ is the transition matrix at time t, describing the change of the system state of all particles in the model from $t - \Delta t$ to t. As the exchange process is stochastic, the transition matrix applied to every update is not constant but dependent on the randomly selected collision particle pairs. The stochastic transition matrix is formally written as follows,

$$\mathbf{P}_t = \mathbf{I}_N - \sum_{l_A,l_P} \left(\mathbf{e}_{l_A}K_A - \mathbf{e}_{l_P}K_P\right)\left(\mathbf{e}_{l_A} - \mathbf{e}_{l_P}\right)^T \tag{8}$$

where $\mathbf{I}_N$ is the identity matrix. Indices l_A and l_P represent the label of all selected particles and corresponding neighbours at time t, respectively. $\mathbf{e}_{l_A}$ (resp. $\mathbf{e}_{l_P}$) denotes the column vector where all entries are 0 except in position l_A (resp. l_P) where the entry is 1. The system state discrete evolution can be expressed by the following form from its initial state,

$$\mathbf{s}(t)^T = \mathbf{s}(0)^T \mathbf{H}^{(t,0)} \tag{9}$$

where $\mathbf{H}^{(t,0)} = \mathbf{P}_{\Delta t}\mathbf{P}_{2\Delta t}\cdots\mathbf{P}_{t-\Delta t}\mathbf{P}_t$ (the right product of a sequence of stochastic matrices) is the so-called *non-homogenous stochastic Markov chain* [14].

The properties of stochastic Markov chain have been extensively studied [15–18]. It is easy to observe that the transition matrix $\mathbf{P}_t$ is a *row-stochastic* matrix in which each row sum is equal to 1. When a stochastic Markov chain formed of such matrices is long enough, (i) its *ergodic property* [15] shows that the long-term system state will be independent of its initial state and (ii) its result is almost identical to the average of the ensemble of simulations. According to Tahbaz-Salehi and Jadbabaie [16], the stochastic chain $\mathbf{H}^{(t,0)}$ can always lead to convergence when t is large enough because all of the particles are connected in the exchange network with no isolated component, showing

$$\mathbf{H}^{(t,0)} = \mathbf{1}\mathbf{d}(t)^T \tag{10}$$

where $\mathbf{1}$ is an N-by-1 column vector where all entries are 1 and $\mathbf{d}(t)^T$ is the distribution vector at time t that describes the asymptotic system state after long-run process. To characterise the system state, the variance of material distribution is defined as

$$\sigma(t)^2 = \frac{1}{N}\left|\left|\mathbf{s}(t) - m_{\text{avr}}\mathbf{1}\right|\right|^2 \tag{11}$$

where m_{avr} is the average material amount and $||\cdot||$ is the euclidean norm of vector. Combining Equations (9) to (11), we have the following expression for the coefficient of variation of material distribution in the stochastic model,

$$CoV(t) = \left(||\mathbf{d}||^2 N - 1\right)^{0.5} \tag{12}$$

It is observed that once the particle population is given, $CoV(t)$ is only dependent on the distribution vector $\mathbf{d}$. For a Markov chain that has constant stochastic matrix at each step, the system would eventually achieve an equilibrium with deterministic convergence and constant distribution vector [19]. In our collision-exchange system, however, the stochastic matrix $\mathbf{P}_t$ at each iteration is stochastic, which results in a random convergence and an uncertain distribution vector [20, 21] that are significantly dependent on the sequence of stochastic matrices. According to Tahbaz-Salehi and Jadbabaie [18], the asymptotic state that the system will approach is a distribution with non-zero variance. The mean of variance at steady state is determined by

$$\mathbf{K}vec\left(\mathbf{I}_N\right) = \mathbb{E}(||\mathbf{d}||^2)\, vec\left(\mathbf{1}_{N\times N}\right) \tag{13}$$

where

$$\mathbf{K} = \lim_{t\to\infty}\left[\mathbb{E}\left(\mathbf{P}_k \otimes \mathbf{P}_k\right)\right]^t \tag{14}$$

where $\otimes$ denotes the Kronecker product, $vec(\cdot)$ is the vectorisation by stacking columns of a matrix into a single column vector.

Let us give illustrative examples of the results computed using Markov chain analysis (Equations (11) and (12)) and obtained from stochastic simulations (using simulation algorithm in Section 2.1), to present the impact of the conditions and parameters on the model outputs.

Table 1 shows the comparisons of analytical expected values and simulation averages of material distribution with different model conditions and parameters. From the table, the stochastic simulation outputs completely agree with the Markov analysis results. The discrepancies between $\mathbb{E}(\sigma)$ and $\overline{\sigma}$ (as well between $\mathbb{E}(CoV)$ and $\overline{CoV}$) in all examples are acceptable as the fluctuation of numerical simulation realisation is inevitable due to the model stochasticity. In Table 1, it is observed from models No.1 to 4 that the expected σ and CoV of material distribution weakly depend on the particle population for the same transfer coefficients $K_A = 0.72$ and $K_P = 0.26$. The slight change of expected σ (or expected CoV) is caused by the increasing number of particles in the system because the same transfer coefficients would make the coating material distributed more raggedly in a system with larger particle population. This result agrees with what has been presented in Huang et al. [22].

Models No.4 to 6 are constructed with the same particle population $K = 60$ but different dimensionality, i.e. 1D, 2D and 3D, respectively. The results show that once transfer coefficients and number of particles are fixed in the model, the system always tends to the same asymptotic state as described by the analytic solution, no matter what dimensionality the model applies. This implies that when the process time is large enough the material distribution at steady state is theoretically not related to the system geometry. From an industrial point of view, using vessels with different geometries would yield similar results of material distribution for the same amount of material and the same number of particles.

Table 1: Standard deviation and coefficient of variation of material distribution at steady state calculated by formula and by numerical simulation averages for $m_{\text{avr}} = 50$.

No.	Population dimensions	Transfer coefficient (particle)	Transfer coefficient (neighbour)	Expected value		Numerical simulation average	
(-)	(K_x, K_y, K_z)	K_A	K_P	$\mathbb{E}(\sigma)$	$\mathbb{E}(CoV)$	$\overline{\sigma}$	$\overline{CoV}$
1	(30,1,1)	0.72	0.26	35.71	0.714	34.44	0.689
2	(40,1,1)	0.72	0.26	35.94	0.719	34.13	0.683
3	(50,1,1)	0.72	0.26	36.08	0.722	33.57	0.676
4	(60,1,1)	0.72	0.26	36.17	0.723	32.73	0.655
5	(12,5,1)	0.72	0.26	36.17	0.723	34.23	0.685
6	(5,4,3)	0.72	0.26	36.17	0.723	33.85	0.677
7	(5,4,3)	0.91	0.18	74.13	1.483	66.87	1.337
8	(5,4,3)	0.50	0.25	18.72	0.374	16.99	0.340
9	(5,4,3)	0.62	0.37	18.09	0.362	16.58	0.332
10	(5,4,3)	0.54	0.45	6.34	0.127	6.35	0.127
11	(5,4,3)	0.52	0.49	2.10	0.042	2.07	0.041
12	(5,4,3)	0.42	0.42	0	0	0	0

In models No.6 to 11, the results are compared using the same population dimension for the different values of the transfer coefficients given by Table 1. It is observed that σ and CoV of material distribution are significantly influenced by the difference between K_A and K_P. For smaller differences, σ and CoV decrease, indicating that the material is distributed more evenly in the system. In model No.12, the model condition is set as $K_A = K_P$. In the result, $\sigma = CoV = 0$ implies that the system achieves a state where all particles have identical amount of coating material. With the condition of $K_A = K_P$, the transition matrix $\mathbf{P}_t$ is known as a *doubly-stochastic* matrix where both row sum and column sum are equal to 1. The stochastic Markov chain $\mathbf{H}^{(t,0)}$ will consequently always lead to a distribution vector in which all entries are identical [15, 16].

Analytically computing the expected value of $||\mathbf{d}||^2$ allows to see the average material distribution behaviour at steady state instead of repeating simulation multiple times with the same input variables. However, the computational burden on a system with a large particle population will be terribly high as the size of stochastic matrix $\mathbf{P}_t$ will be squared after Kronecker multiplication and $vec(\cdot)$ also yields vectors of dreadful size. This problem can be solved by using a regression fitting method with respect to N and $||\mathbf{d}||^2$.

b. Deterministic model approximation

In Section 2.1.1 a, we have discussed the long-term system state and the distribution of coating materials in the particle collision-exchange model. In this section, we study the deterministic evolution of system state. The system is simulated by using the SSA illustrated in Section 2.1. Re-running a stochastic simulation with the same input condition would almost surely not reproduce the realisation due to model stochasticity. Even though stochastic simulations present the system uncertainty, one still expects to see the *average* emergent dynamic behaviour of the system.

Any particle (i, j, k) in the system will randomly experience one of the following three situations in a simulation time step.

(1) Particle (i, j, k) involved in an exchange event associated with the transfer coefficient K_A. In this situation, the particle state $m^{(1)}_{i,j,k}(t + \Delta t)$ is determined by Equation (4). The probability of occurrence of situation (1) is defined as

$$P^{(1)} = N^{-1} P^{\mathbf{e}}_{i,j,k} \Delta t \tag{15}$$

(2) Particle (i, j, k) involved in an exchange event associated with the transfer coefficient K_P. In this situation, the particle state is written as

$$m^{(2)}_{i,j,k}(t+\Delta t) = m_{i,j,k}(t)(1-K_P)+m_{(i,j,k)+\mathbf{e}}(t)K_A \tag{16}$$

The probability of occurrence of situation (2) is defined as

$$P^{(2)} = N^{-1} P^{-\mathbf{e}}_{(i,j,k)+\mathbf{e}} \Delta t \tag{17}$$

(3) Particle (i, j, k) not involved in any exchange event during Δt. In this situation, the particle state will keep

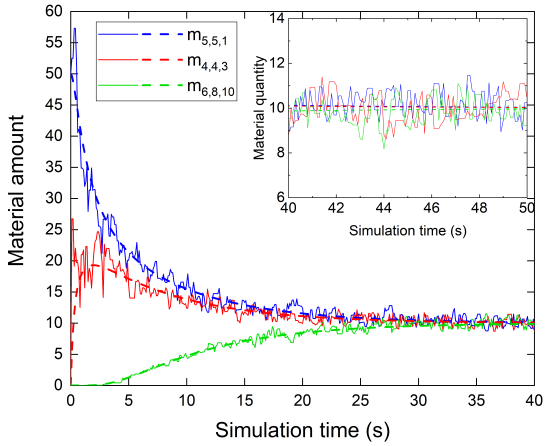

(a)

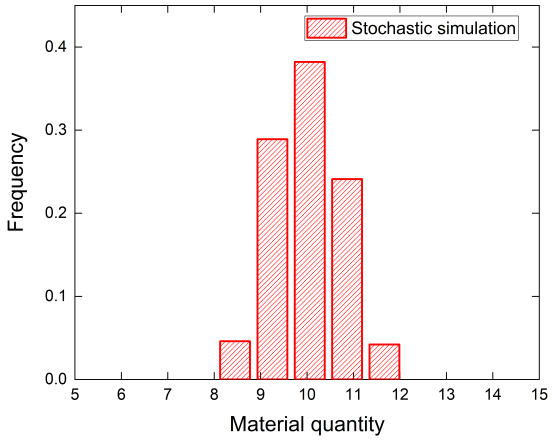

(b)

Figure 3: (a) Comparison between stochastic realisation and deterministic evolution of material amount on particles and (b) material amount distribution in the stochastic model at $t = 50s$ for $K_x = K_y = K_z = 10$, $N = 1000$, $m_{\text{avr}} = 10$, $K_A = 0.5$, $K_P = 0.45$, $c_f = 8000s^{-1}$, $\Delta t = 0.01s$, $P^{\mathbf{e}}_{i,j,k} = 1/6$. Initially only the particles on the top two layers have identical amount of material. The solid lines represent the stochastic realisations of the particles and the dashed lines represent the deterministic evolution of the corresponding particles with the same colour.

unchanged so we have

$$m^{(3)}_{i,j,k}(t + \Delta t) = m_{i,j,k}(t) \tag{18}$$

The probability of occurrence of situation (3) is defined as

$$P^{(3)} = 1 - P^{(1)} - P^{(2)} \tag{19}$$

By using addition and multiplication laws of probability theory, we derive the stochastic mean of the state of particle (i, j, k) at time $t + \Delta t$:

$$\begin{aligned} m_{i,j,k}(t + \Delta t) = {} & P^{(1)} m^{(1)}_{i,j,k}(t + \Delta t) \\ & + P^{(2)} m^{(2)}_{i,j,k}(t + \Delta t) \\ & + P^{(3)} m^{(3)}_{i,j,k}(t + \Delta t) \end{aligned} \tag{20}$$

The collision propensities $P^{\mathbf{e}}_{i,j,k}$ are crucial to determine how Equation (20) can be further simplified and solved. For systems with homogeneous isotropic turbulence, it is plausible to assume that a particle has the same possibility to collide with one of its neighbours, that is to say, the particle collision is non-diagonally isotropic that all $P^{\mathbf{e}}_{i,j,k}$ are identical, Equation (20) can be simplified into the following form:

$$\frac{dm_{i,j,k}}{dt} = \left(\sum_{(i,j,k)+\mathbf{e} \in I_{all}} m_{(i,j,k)+\mathbf{e}} - R\, m_{i,j,k} \right) (K_A + K_P) \frac{c_f}{N} P^{\mathbf{e}}_{i,j,k} \tag{21}$$

where R is the number of valid non-diagonal neighbours with respect to the (i, j, k)-th particle, depending on the particle position.

Equation (21) is expected to describe the deterministic time evolution of the material amount on the (i, j, k)-th particle. Figure 3 compares the stochastic simulation realisation by using the SSA and deterministic system evolution by using Equation (21), with model inputs and initial condition listed in the caption.

Figure 3(a) gives an example of the good agreement between stochastic realisation (solid lines) and corresponding deterministic evolution (dashed lines) with respect to the material amount over individual particles. For clarity, we plotted the time evolution of three particles at different positions in the system. The material is transferred between particles and gradually spread throughout the entire system. The dashed lines converge at around 40 seconds, indicating that the system is approaching the steady state. Afterwards it is observed

Table 2: Summary of modelling approaches characterising the system evolution

	Stochastic process	Deterministic mean field
Assumptions	• Unchanged order of members • Binary collisions in non-diagonal directions only • Linear liquid transfer mechanism • Constant model parameters • No material quantity loss after a collision with model boundary	• All assumptions in Stochastic process • Identical collision propensity (non-diagonally isotropic process)
Strength	• Expected uncertainty of material distribution • Revealing the relationship between parameters and uncertainty on material distribution • Suitable for identifying material distribution uncertainty in specific systems with small population size	• Expected material quantity on individuals • Allowing deterministic sensitivity analysis and experimental design with explicit model expression • Suitable for approximately identifying transient behaviour of system
Limitation	• High computational burden for large population size	• Material distribution not investigated at steady state

from the solid lines that the individual particle material amount no longer dramatically varies but fluctuates around the average value m_{avr}. The deterministic approximation represents the mean field of the particle states, summarised based on all potentials at the same time. This mean field approximation allows an explicit model expression to be used for further studies, which would save computational time in performing sensitivity analysis and designing experiments.

However, the deterministic mean field evolution is limited because it cannot predict any coefficient of variation or material distribution at steady state which can instead be obtained from stochastic simulations such as the one shown in Figure 3(b) obtained at $t = 50s$ in stochastic simulation. This limitation may be relaxed in the future by adding noise terms derived from the system uncertainty to the deterministic expression, forming stochastic differential equations.

Table 2 summarises the modelling approaches characterising the system evolution discussed in Section 2.1.1. In order to investigate the potential of the collision-exchange stochastic model, in Section 3, we will present an illustrative example of seed coating process to discuss how we can fit the collision-exchange stochastic model to understand the seed coating process.

3 Model application

In this section, a simple collision-based real system is studied applying the 3D compartment model in order to investigate feasibility, potential and possible issues. The physical process selected as a test case is seed coating.

3.1 Seed coating process

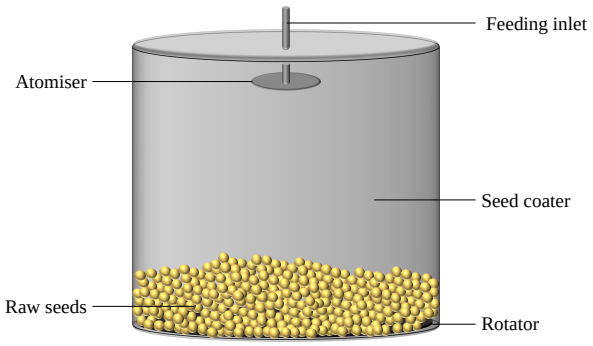

Figure 4: Sketch of the seed coating system

In agrochemical industry, seed coating is a vital unit operation where raw seeds are coated by some chemical agent that reinforces seed growth performance and protects seeds from being damaged and contaminated by ambient surroundings. This process is affected by several factors such as seed shape, surface texture, property of chemical agent and coating vessel configuration. The seeds are mixed with a coating agent in a batch coater whose geometry is shown as in Figure 4 More details on coater geometry, coating variability, and relevant studies have been summarised [23].

The operating conditions of the seed coating process

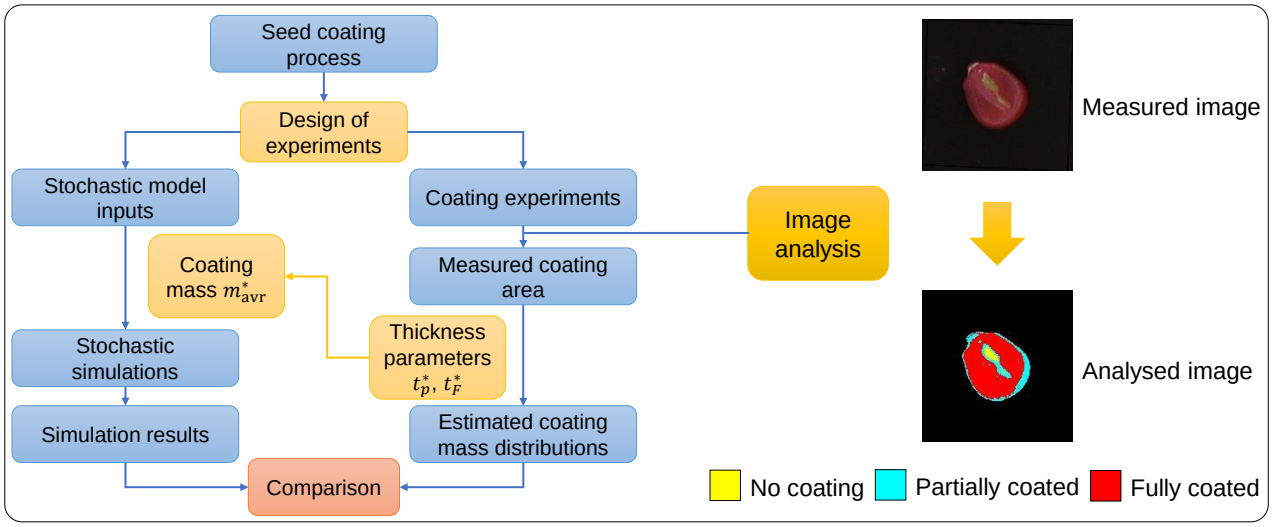

Figure 5: Flowchart for seed coating distribution measurement and estimation by using image analysis and nominal thickness parameters t^*_P, t^*_F.

consist of seed loading mass, coating formulation loading mass, average seed size, average seed mass, post-mixing time and spray droplet size. Average seed size refers to the average diameter of the seeds to be coated. For seeds of irregular shape, the geometric mean diameter would be considered. Post-mixing time represents the mixing time applied after the coating agent is completely added to the system.

3.2 Seed coating experiment

In the experiment, the coating amount on seed surface is measured and compared to the stochastic simulation results. Figure 5 presents the flowchart of experiment design, stochastic simulations and seed coating distribution measurement and estimation.

The operating conditions of experiments are obtained based on Response Surface Methodology (RSM) in Design of Experiments (DoE) [24], generating seven experiments with experimental settings of different coating agent amounts and post-mixing times. The input variables of stochastic simulations are determined as follows,

- Particle population, N: determined by the seed loading mass and the average seed mass in the system. One kilogram of corns is applied in each run which approximates more than 3000 number of seeds.
- Population dimensions, (K_x, K_y, K_z): determined by the seed coater geometry, the average seed size and the pattern of seed bed, see Figure 6. In the coater, when the rotator is on, the seeds fed into the coating chamber tend to stay away from the centre of the floor and gather at the wall due to the effects of strong centrifugal force and inevitable gravitational force. When the moving seed bed becomes stable, the bed forms a hollow cylinder with very limited number of seeds escaping from the bulk.
- Average amount of material, m_{avr}: assigned based on the average estimated coating amount m^*_{avr} to be mentioned later;
- Initial distribution: the stochastic Markov analysis in Section 2.1.1 suggests that all particles (seeds) can be assumed to initially have identical amount of material, i.e. m^*_{avr}, when one focuses only on final distribution. However, if one wants to investigate the dynamic behaviour of the system, the initial distribution should be consistent with realistic situations.

Image analysis is applied to obtain the coating area to measure the coating distribution at steady state. The coated seeds are captured by camera and then the images are analysed to give the data that describes the coating coverage on seed surface. As seen from Figure 5, the analysed image shows three distinct colours, which represent the different degrees of adsorption of coating agent. The red region represents the area is fully coated. The cyan region represents the area is partially coated. And the yellow region represents no coating observed in the area. Assuming a uniform coating thickness in every region allows to convert the coating area distribution into estimating coating mass distribution by introducing

Table 3: Seed coating experimental results and corresponding stochastic simulation realisations for $t_P^* = 0.5$ and $t_F^* = 1$.

No.	Experiments				Simulations				
	Coating agent fed (g)	Post-mixing time (s)	Sample stddev $(\sigma_1^*,\sigma_2^*,\sigma_3^*)$	Sample CoV $(CoV_1^*,CoV_2^*,CoV_3^*)$	Average coating mass m_{avr}^*	Expected stddev $\mathbb{E}(\sigma)$	Expected CoV $\mathbb{E}(CoV)$	Transfer coefficient K_A	Transfer coefficient K_P
1	2.80	20	(549.8, 477.3, 513.0)	(0.609, 0.582, 0.632)	845.3	528.4	0.625	0.60	0.20
2	8.25	60	(460.4, 514.6, 450.4)	(0.134, 0.150, 0.130)	3443.0	438.1	0.127	0.50	0.41
3	17.70	20	(473.2, 476.7, 426.2)	(0.114, 0.116, 0.102)	4144.6	467.9	0.113	0.50	0.42
4	24.30	60	(454.0, 470.6, 479.5)	(0.106, 0.110, 0.112)	4277.6	452.8	0.106	0.495	0.42
5	30.45	20	(450.1, 469.9, 473.1)	(0.107, 0.111, 0.113)	4206.4	474.9	0.113	0.50	0.42
6	8.25	40	(451.1, 487.9, 516.6)	(0.129, 0.141, 0.145)	3510.8	496.2	0.141	0.50	0.40
7	8.25	20	(435.8, 534.5, 480.9)	(0.127, 0.155, 0.137)	3467.7	440.3	0.127	0.50	0.41

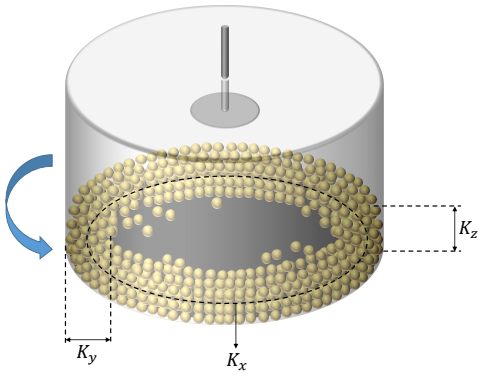

Figure 6: Sketch of the seed bed forming a hollow cylinder during coating process.

nominal thickness parameters t_P^* and t_F^* for the partially and the fully coated regions, respectively. The coating mass on a single seed is therefore determined by

$$m^* = t_P^* n_P + t_F^* n_F \tag{22}$$

where n_P (resp. n_F) corresponds to the number of pixels in the partially (resp. fully) coated region of projected area.

It is worth noting that using different values of t_P^* and t_F^* would not affect the comparison between simulation realisations and experimental results. This is because t_P^* and t_F^* affect m^* linearly and therefore m_{avr}^*. That is to say, using different values of t_P^* and t_F^* would only alter the locations (mean value) of distribution curves of stochastic realisations and experimental results but not change their distribution pattern. Additionally, m_{avr}^* would have no impact on the value of CoV_{material} due to Equation (12). In what follows, the experimental results would be compared to the stochastic simulations with $t_P^* = 0.5$ and $t_F^* = 1$.

3.3 Model verification

In this section, we identify the impact of different experiment operating conditions by taking proper values of K_A and K_P in stochastic simulations which give similar coating material distributions.

Table 3 on the left shows the seed coating experimental results with different amount of coating agent fed and post-mixing time applied and on the right presents the simulation outputs based on the stochastic collision-exchange model. For each experiment, three sample sets of the coated seeds are measured to show the standard deviation and coefficient of variation. In Table 3, the values of transfer coefficients were estimated to ensure we could obtain simulated material distributions that would agree with experiments in terms of mean, variance and distribution pattern.

Figures 7(a) to 7(g) illustrate the comparisons between experimental results and stochastic simulation realisations with respect to the estimated coating mass distribution, which shows how this model is capable of reproducing observed experimental results, with the appropriate coefficients selected. Figure 7(h) illustrates the comparison between coating mass distributions of different amounts of coating agent. Figure 7(i) illustrates the comparison between coating mass distributions of different post-mixing times. Experiments No.2 to 5 give the bell-shaped distributions which can be reproduced by the simulations with model parameters $K_A = 0.50$ ($K_A = 0.495$ in experiment No.4) and $K_P = 0.42$ ($K_P = 0.41$ in experiment No.2). Experiment No.1 gives the exponential-like distribution which can be reproduced by the simulation with $K_A = 0.60$ and $K_P = 0.20$. The observed coating mass distribution in the experiments is anticipated to be described by the model parameters K_A and K_P. From Figure 7(h), in experiments No.2 to 5, the higher amount of coating agent was fed into the

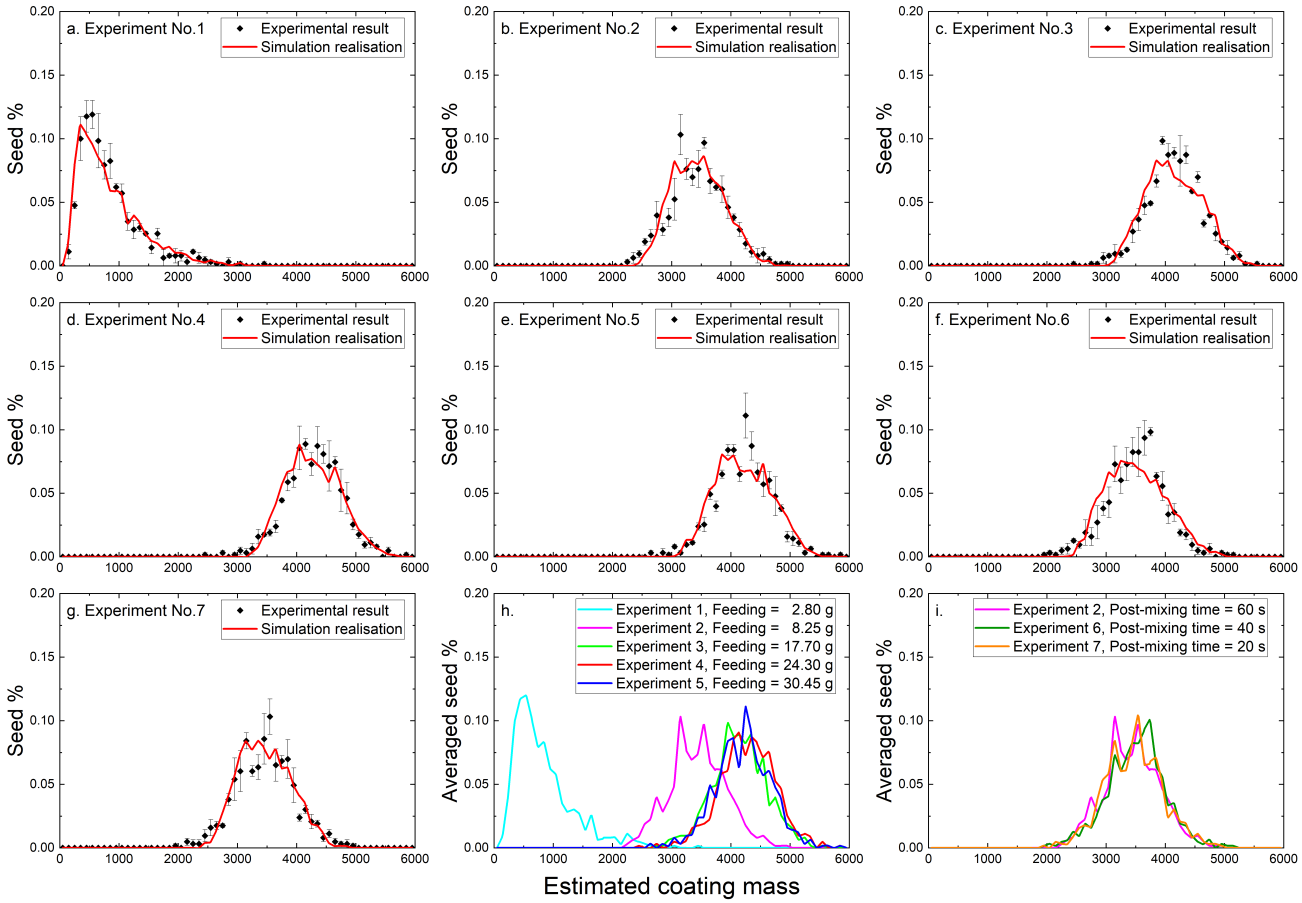

Figure 7: (a) to (g) Comparisons between seed coating experimental results and simulation outputs for experiments No.1 to 7. Model conditions: $(K_x, K_y, K_z) = (60, 10, 5)$, i.e. $N = 3000$, $c_f = 9000s^{-1}$, $dt = 0.01s$, $P^{\mathbf{e}}_{i,j,k} = 1/6$, $t^*_P = 0.5$ and $t^*_F = 1$; (i) Comparison between coating mass distributions of different amounts of coating agent; (h) Comparison between coating mass distributions of different post-mixing times.

system so that the liquid was easily transferred between the seeds, leading to a better coating distribution, described by two close values of K_A and K_P. In experiment No.1, using coating agent of 2.8 g leads to a poor liquid transfer between the seeds as inadequate coating liquid on seed surface makes it hard for other seeds to capture coating from it, which is reflected by the large difference between K_A and K_P. Estimating the model parameters K_A and K_P with experiment operating conditions can characterise the coating behaviour in the experiment. K_A and K_P can be influenced by several factors in the coating system, including seed surface texture, coating liquid density and coating liquid viscosity. Investigating K_A and K_P by varying these properties allows to understand their impacts on the coating result.

In Figure 7(i), the results of experiments No.2, 6 and 7 are presented as distributions with different colours. Experiments No.2, 6 and 7 applied the same amount of coating agent but different post-mixing times. Experiments No.2, 6 and 7 are designed to verify the steady state that the seed coating system can achieve after a certain period of time. As seen from the figure, as well as the values of K_A and K_P, there is no big variation among the samples, indicating that the seed coating distribution does not significantly evolve with time any longer after post-mixing time larger than 20 seconds. The actual post-mixing time threshold, i.e. the minimum post-mixing time required for system to reach steady state, can be even smaller and its effect will be analysed more in details in the future.

Experiments No.3, 4 and 5 applied very different amount of coating agent but it is observed that these three experiments present very similar coating result in terms of the distribution pattern and the average coating mass m^*_{avr}. This phenomenon can be explained by two aspects. (1) After discharging the coated seeds, the residual coating

agent left in the coater in experiment No.5 was much more than that observed in experiment No.1. This indicates that there exists a maximum capability for seeds to keep coating adsorbed on surface as it would be increasingly hard for seed surface to receive excessive coating agent when the surface has been gradually occupied. As more coating agent fed into the system, the final coating distribution would approach asymptotically to an upper limit. The maximum capability of holding coating liquid for seeds will be inserted in the model in a future version to present stochastic simulation outputs with higher precision. (2) Introducing nominal thickness parameters t_P^* and t_F^* artificially is equivalent to assuming that the real coating thickness is uniform in fully coated region and this approximation may ignore the existence of the potential multilayer coating on seed surface, leading to an artificial upper bound of m_{avr}^* which might be lower than the real maximum capability. High-performance liquid chromatography (HPLC) will be applied in the future to precisely measure the coating amount on seed surface.

The promising agreement on the coating material distribution between experimental results and stochastic simulation outputs shows how this modelling approach is applicable and the flexibility of the proposed modelling approach. It is worth noting that the presented K_A-K_P pairs in the results are not the only choice to give similar distributions. In this work, the value of K_A is chosen to be around 0.5 which is convenient for us to compare the influence of K_A-K_P differences on the results. According to Equation (21), K_A and K_P influence the system dynamics in the coating process. Taking samples at different time points would facilitate estimating the actual values of K_A and K_P. Rigorous parameter estimation requires strategies for uncertain sampling in experiments and optimisation with uncertainty in stochastic models, and it will be the subject of a separate work.

4 Conclusion

A compartment stochastic model is developed in this paper, aiming to simulate the particle collision-exchange system. The implemented SSA allows to compute the state evolution in the collision-exchange system with less computational intensity.

The discrete Markov process associated with the stochastic model is studied. The analytical results present the average long-term state in the collision-exchange system that is independent of model population, model dimensionality and model initial condition. The deterministic mean field analysis presents the average evolution with respect to the material amount on each single particle, computed based on all potential states of a particle at the same time.

The application of the model to the investigation of mass distribution in the seed coating process is promising because the coating system can be identified and described by the accessible model parameters. This work also shows that this model can support identification of basic physics of the collision-exchange process in the system.

Future work will aim to develop the model considering dynamics, particle motion and simulation efficiency, and to attempt global sensitivity analysis and parameter estimation for the stochastic model. The former will enable the model to predict the collision-exchange system evolution with high accuracy, while the latter aims to identify the impact of uncertainty on model outputs and understand the model-based design of experiment for stochastic models.

Acknowledgements

The authors gratefully acknowledge the support of the Department of Chemical Engineering, University College London and Syngenta. The authors would like to thank Emily Kynaston from Syngenta for the help and support on the experiments.

Nomenclature

Alphabetical letters

c_f	Contact frequency (s^{-1})
E	Exchange direction set
$\mathbb{E}(\cdot)$	Analytical average or Expected value
I_{all}	Compartment index set
K	Total number of elements
K_x	Number of compartments in x direction
K_y	Number of compartments in y direction
K_z	Number of compartments in z direction
K_A	Transfer coefficient for reference particle
K_P	Transfer coefficient for neighbour particle
m_{avr}	Average material quantity over particles
$m_{i,j,k}(t)$	Material quantity on the (i,j,k)-th particle at time t
m^*	Estimated coating mass on seed surface
m_{avr}^*	Estimated average of coating mass over particles
N	Number of particles
$N_{i,j,k}$	Set of neighbours for the (i,j,k)-th particle
n_F	Number of pixels in fully coated region
n_P	Number of pixels in partially coated region
$P_{i,j,k}^{\mathbf{e}}$	Collision propensity for the (i,j,k)-th particle

R	Number of valid non-diagonal neighbours
t_F^*	Nominal thickness parameter for fully coated region
t_P^*	Nominal thickness parameter for partially coated region
T_{total}	Total simulation time (s)

Vectors and Matrices [dimension]

$\mathbf{d}(t)$	Distribution vector at time t $[N]$
$\mathbf{e}$	Exchange direction $[3]$
$\mathbf{e}_{l_A}$	Column vector
$\mathbf{e}_{l_P}$	Column vector
$\mathbf{H}^{(t,0)}$	Stochastic Markov chain from 0 to t $[N \times N]$
$\mathbf{M}_0$	Initial material distribution $[N]$
$\mathbf{P}_t$	Stochastic transition matrix at time t $[N \times N]$
$\mathbf{s}(t)$	System state at time t $[N]$

Greek letters

Δt	Numerical computational time interval
$\sigma(t)$	Standard deviation of material distribution at time t
$\bar{\sigma}$	Numerical average of σ
σ^*	Coating mass standard deviation of sample seeds

Acronyms

CoV	Coefficient of variation
DEM	Discrete element method
DoE	Design of experiments
RSM	Response surface methodology
SSA	Stochastic simulation algorithm
TTEP	Travelling traders' exchange process

References

[1] Pierre Gaspard and Thomas Gilbert. On the derivation of fourier's law in stochastic energy exchange systems. *Journal of Statistical Mechanics: Theory and Experiment*, 2008(11):P11021, 2008.

[2] Shweta Bansal, Bryan T Grenfell, and Lauren Ancel Meyers. When individual behaviour matters: homogeneous and network models in epidemiology. *Journal of the Royal Society Interface*, 4(16):879–891, 2007.

[3] Babacar Mbaye Ndiaye, Lena Tendeng, and Diaraf Seck. Comparative prediction of confirmed cases with covid-19 pandemic by machine learning, deterministic and stochastic sir models. *arXiv preprint arXiv:2004.13489*, 2020.

[4] Daniel T Gillespie. Exact stochastic simulation of coupled chemical reactions. *The journal of physical chemistry*, 81 (25):2340–2361, 1977.

[5] Steven S Andrews and Dennis Bray. Stochastic simulation of chemical reactions with spatial resolution and single molecule detail. *Physical biology*, 1(3):137, 2004.

[6] Deliang Shi and Joseph J McCarthy. Numerical simulation of liquid transfer between particles. *Powder Technology*, 184(1):64–75, 2008.

[7] Sarbaz HA Khoshnaw, Muhammad Shahzad, Mehboob Ali, and Faisal Sultan. A quantitative and qualitative analysis of the covid–19 pandemic model. *Chaos, Solitons & Fractals*, 138:109932, 2020.

[8] Ben Freireich and Carl Wassgren. Intra-particle coating variability: analysis and monte-carlo simulations. *Chemical Engineering Science*, 65(3):1117–1124, 2010.

[9] Arjun Kalbag and Carl Wassgren. Inter-tablet coating variability: tablet residence time variability. *Chemical Engineering Science*, 64(11):2705–2717, 2009.

[10] Chunlei Pei, Hungyen Lin, Daniel Markl, Yao-Chun Shen, J Axel Zeitler, and James A Elliott. A quantitative comparison of in-line coating thickness distributions obtained from a pharmaceutical tablet mixing process using discrete element method and terahertz pulsed imaging. *Chemical Engineering Science*, 192:34–45, 2018.

[11] Alberto Di Renzo and Francesco Paolo Di Maio. Comparison of contact-force models for the simulation of collisions in dem-based granular flow codes. *Chemical engineering science*, 59(3):525–541, 2004.

[12] Colin Thornton, Sharen J Cummins, and Paul W Cleary. An investigation of the comparative behaviour of alternative contact force models during elastic collisions. *Powder Technology*, 210(3):189–197, 2011.

[13] Sean P Meyn and Richard L Tweedie. *Markov chains and stochastic stability*. Springer Science & Business Media, 2012.

[14] John Hajnal and MS Bartlett. Weak ergodicity in non-homogeneous markov chains. In *Mathematical Proceedings of the Cambridge Philosophical Society*, volume 54, pages 233–246. Cambridge University Press, 1958.

[15] John Hajnal and MS Bartlett. The ergodic properties of non-homogeneous finite markov chains. In *Mathematical Proceedings of the Cambridge Philosophical Society*, volume 52, pages 67–77. Cambridge University Press, 1956.

[16] Alireza Tahbaz-Salehi and Ali Jadbabaie. A necessary and sufficient condition for consensus over random networks. *IEEE Transactions on Automatic Control*, 53(3):791–795, 2008.

[17] Behrouz Touri and Angelia Nedic. On ergodicity, infinite flow, and consensus in random models. *IEEE Transactions on Automatic Control*, 56(7):1593–1605, 2011.

[18] Alireza Tahbaz-Salehi and Ali Jadbabaie. Consensus over ergodic stationary graph processes. *IEEE Transactions on automatic Control*, 55(1):225–230, 2010.

[19] Lin Xiao and Stephen Boyd. Fast linear iterations for distributed averaging. *Systems & Control Letters*, 53(1): 65–78, 2004.

[20] Stephen Boyd, Arpita Ghosh, Balaji Prabhakar, and Devavrat Shah. Randomized gossip algorithms. *IEEE/ACM Transactions on Networking (TON)*, 14 (SI):2508–2530, 2006.

[21] Fabio Fagnani and Sandro Zampieri. Randomized consensus algorithms over large scale networks. *IEEE Journal on Selected Areas in Communications*, 26(4): 634–649, 2008.

[22] Chunbing Huang, Patrick M. Piccione, Federica Cattani, and Federico Galvanin. Traveling traders' exchange problem: Stochastic modeling framework and two-layer model identification strategy. *Industrial & Engineering Chemistry Research*, 57(30):10011–10025, 2018.

[23] Mehrdad Pasha, Colin Hare, Mojtaba Ghadiri, Alfeno Gunadi, and Patrick M Piccione. Inter-particle coating variability in a rotary batch seed coater. *Chemical Engineering Research and Design*, 120:92–101, 2017.

[24] C Montgomery Douglas et al. Design and analysis of experiments. *John Wiley and sons*, 2001.